

Ultrafast selective extraction of hot holes from cesium lead iodide perovskite films

著者	Shen Qing, Ripolles Teresa S., Even Jacky, Zhang Yaohong, Ding Chao, Liu Feng, Izuishi Takuya, Nakazawa Naoki, Toyoda Taro, Ogomi Yuhei, Hayase Shuzi
journal or publication title	Journal of Energy Chemistry
volume	27
number	4
page range	1170-1170
year	2018-01-16
URL	http://hdl.handle.net/10228/00007533

doi: info:doi/10.1016/j.jechem.2018.01.006

Ultrafast selective extraction of hot holes from cesium lead iodide perovskite films

Qing Shen^{a,*}, Teresa S. Ripolles^{b,*}, Jacky Even^{c,*}, Yaohong Zhang^a, Chao Ding^a, Feng Liu^a, Takuya Izuishi^a, Naoki Nakazawa^a, Taro Toyoda^a, Yuhei Ogomi^b, Shuzi Hayase^{b,*}

^aDepartment of Engineering Science, Faculty of Informatics and Engineering, The University of Electro-Communications, 1-5-1 Chofugaoka, Chofu, Tokyo 182-8585, Japan

^bGraduate School of Life Science and Systems Engineering, Kyushu Institute of Technology, 2-4 Hibikino, Wakamatsu, Kitakyushu 808-0196, Japan

^cFonctions Optiques pour les Technologies de l'information, UMR 6082, INSA, 35708 Rennes, France

Corresponding authors.
shen@pc.uec.ac.jp

(Q. Shen), teresa@life.kyutech.ac.jp (T. S. Ripolles), jacky.even@insa-rennes.fr (J. Even), hayase@life.kyutech.ac.jp (S. Hayase).

KEYWORDS: CsPbI₃; Perovskite; Hot carrier cooling; Hot hole transfer; Hot phonon bottleneck

ABSTRACT: Lead halide perovskites have some unique properties which are very promising for

optoelectronic applications such as solar cells, LEDs and lasers. One important and expected application of perovskite halide semiconductors is solar cell operation including hot carriers. This advanced solar cell concept allows overcoming the Shockley–Queisser efficiency limit, thereby achieving energy conversion efficiency as high as 66% by extracting hot carriers. Understanding ultrafast photoexcited carrier dynamics and extraction in lead halide perovskites is crucial for these applications. Here, we clarify the hot carrier cooling and transfer dynamics in all-inorganic cesium lead iodide (CsPbI_3) perovskite using transient absorption spectroscopy and Al_2O_3 , poly(3-hexylthiophene-2,5-diyl) (P3HT) and TiO_2 as selective contacts. We find that slow hot carrier cooling occurs on a timescale longer than 10 ps in the cases of $\text{CsPbI}_3/\text{Al}_2\text{O}_3$ and $\text{CsPbI}_3/\text{TiO}_2$, which is attributed to hot phonon bottleneck for the high photoexcited carrier density. An efficient ultrafast hole transfer from CsPbI_3 to the P3HT hole extracting layer is observed. These results suggest that hot holes can be extracted by appropriate selective contacts before energy dissipation into the halide perovskite lattice and that CsPbI_3 has a potential for hot carrier solar cell applications.

1. Introduction

Organic-inorganic hybrid perovskite ($\text{CH}_3\text{NH}_3\text{PbI}_3$ (MAPbI₃)) solar cells have attracted more and more attention in recent years, because the perovskite can be simply prepared using solution process at low temperatures (≤ 100 °C) and the record power conversion efficiency (PCE) has been reported to be over 22% [1–22]. The high efficiency results from some unique properties of MAPbI₃ such as a high optical absorption coefficient [23,24], small exciton binding energy [25], long photoexcited carrier lifetimes [26,27] and very small Urbach energy [28]. However, there are some critical issues for perovskite solar cells such as improving the material stability and understanding the degradation mechanisms. All-inorganic cesium lead halide (CsPbI_3) perovskite is nowadays a basic ingredient entering the composition of stable photovoltaic devices [29–34]. In addition, very recently, it was found that phase stabilization could even be reached in pure CsPbI_3 quantum dot solar cells [35].

To further improve the photovoltaic properties, it is very important to understand the basic processes of photoexcited carrier relaxation. Especially, for advanced applications such as hot carrier solar cells [36] and electrically pumped lasers [37,38], ultrafast photoexcited carrier dynamics is the first key. Very recently, we studied hot carrier cooling dynamics in CsPbI_3 using transient absorption (TA) spectroscopy, finding that it becomes slower as the photoexcited carrier density increases. The cooling time is longer than 10 ps when the photoexcited carrier density is larger than $1 \times 10^{18} \text{ cm}^{-3}$, which is attributed to hot phonon bottleneck for high photoexcited carrier densities [39]. Similar slow hot carrier cooling phenomena for larger photoexcited carrier densities were also observed in MAPbI₃ and FAPbI₃ perovskites [40,41]. Therefore, our findings indicate that the inorganic cation Cs has a similar effect on the hot carrier cooling as organic cations (MA or FA) in a perovskite lattice. For hot carrier solar cell applications, the second key is to extract

hot carriers before they relax to the band edges. In this study, we clarify the hot carrier extraction from CsPbI₃ perovskite using the TA technique. Due to the small thicknesses of halide perovskite thin films, slow cooling dynamics gives a unique opportunity to achieve hot carrier extraction before relaxation to the band edges. For that purpose, Al₂O₃, poly(3-hexylthiophene-2,5-diyl) (P3HT) and TiO₂ are used as selective contacts to elucidate how hot hole and hot electron can be transferred from the CsPbI₃ perovskite to contact layers. The ultrafast efficient extraction of hot holes to P3HT within a few 100 fs, appears as the most striking result of the present work.

2. Experimental

CsPbI₃ perovskite samples were deposited on Al₂O₃ (Al₂O₃/CsPbI₃) without and with a P3HT hole extraction layer (Al₂O₃/CsPbI₃/P3HT) [29]. First, mesoporous Al₂O₃ scaffold films were deposited on glass substrates. The alumina solution was diluted in 2-propanol (2:3 by vol.) and spin coated at 2000 rpm for 60 s. Subsequently, the Al₂O₃ substrates were heated at 60 °C for 10 min and 130 °C for 30 min. The Al₂O₃ substrates were then transferred into a glove box and CsPbI₃ films deposited using a one-step solution deposition method [29]. A mixture of CsI and PbI₂ (wt. ratio 1:1) dissolved in DMF with a concentration of 20 wt% was prepared at 60 °C for that purpose until complete dissolution. The Al₂O₃ substrates were pre-heated at 60 °C for 15 min, and an aliquot of the CsPbI₃ solution was spin-coated at 2000 rpm for 30 s, followed by thermal annealing on a hot plate at 60 °C and then 350 °C for 30 min each. Fig. S1 shows the SEM images of the surfaces of the Al₂O₃ substrate and the CsPbI₃ layer, from which we can observe clearly that both the Al₂O₃ substrate and the CsPbI₃ layer are uniform. The hole extraction material, P3HT, was then spin coated from an aliquot at 1000 rpm for 10 s onto the perovskite films at room temperature. The concentration of the P3HT in *o*-dichlorobenzene was 17 mg/mL. The solution was heated for

several hours at 60 °C. The substrates were kept in a petri dish overnight in the dark to allow the solvent to evaporate. The films were then annealed at 130 °C for 10 min. Finally, the substrates were encapsulated with polymethylmetacrylate (PMMA) on a spin coater at 3000 rpm for 60 s in order to isolate the sample from air and keep them stable.

CsPbI₃/TiO₂ samples were prepared by using mesoporous TiO₂ scaffold films. The TiO₂ substrates were prepared with 20 nm of compact TiO₂ blocking layer by atomic layer deposition and 400 nm of mesoporous TiO₂ (mp-TiO₂) by spin coater. The mp-TiO₂ solution was diluted in α -terpineol (1:3 by vol.) for spin coating at 6000 rpm for 30 s. These films were sintered at 470 °C for 30 min. Once the scaffold layers were synthesized, the substrates were transferred into a glove box. Then, CsPbI₃ perovskites were prepared on the TiO₂ films using the method as mentioned above.

A femtosecond TA setup was used to study the photoexcited carrier dynamics, especially the hot carrier cooling dynamics in CsPbI₃ [42–45]. The laser source was a titanium/sapphire laser (CPA-2010, Clark-MXR Inc.) with a wavelength of 775 nm, a repetition rate of 1 kHz, and the pulse width is 150 fs. The light was separated into two parts. One part was incident on a sapphire plate to generate white light for the probe beam. The other part was used to pump an optical parametric amplifier (OPA) (a TOAPS from Quantronix) to generate light pulses to excite the sample. In this study, the pump light wavelength was 470 nm (2.6 eV) and the pump light intensity was 23 $\mu\text{J}/\text{cm}^2$. Time-resolved TA spectra were obtained from 530 nm (2.34 eV) to 750 nm (1.65 eV) with a temporal resolution of about 100 fs. For all measurements, the pump and probe beams were incident on the glass (Al₂O₃/CsPbI₃ or TiO₂/CsPbI₃) side of the samples and the TA measurements were carried out at room temperature.

3. Results and discussion

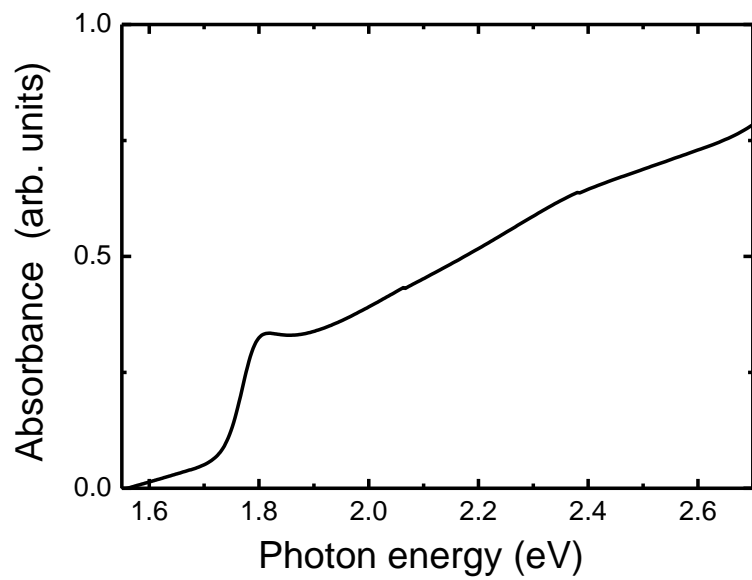


Fig. 1. Typical optical absorption spectrum of CsPbI₃.

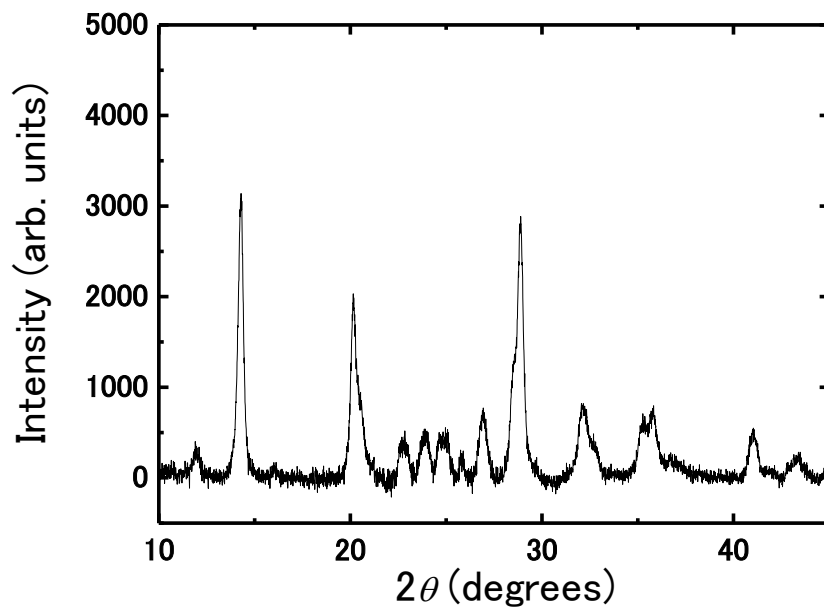
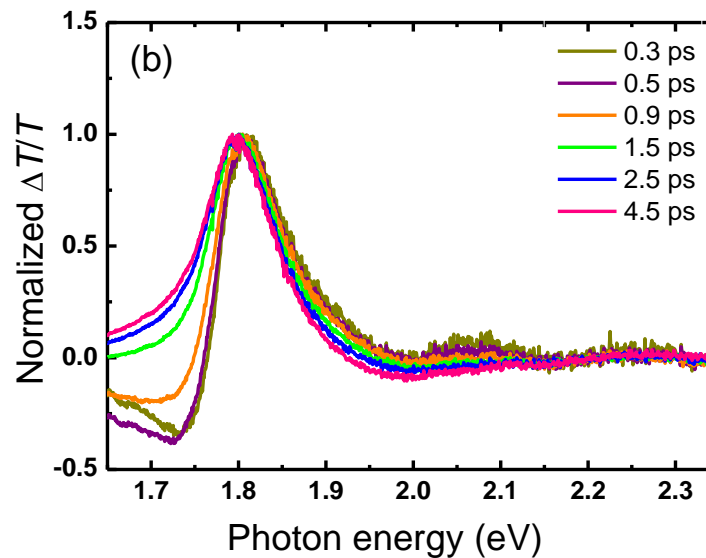
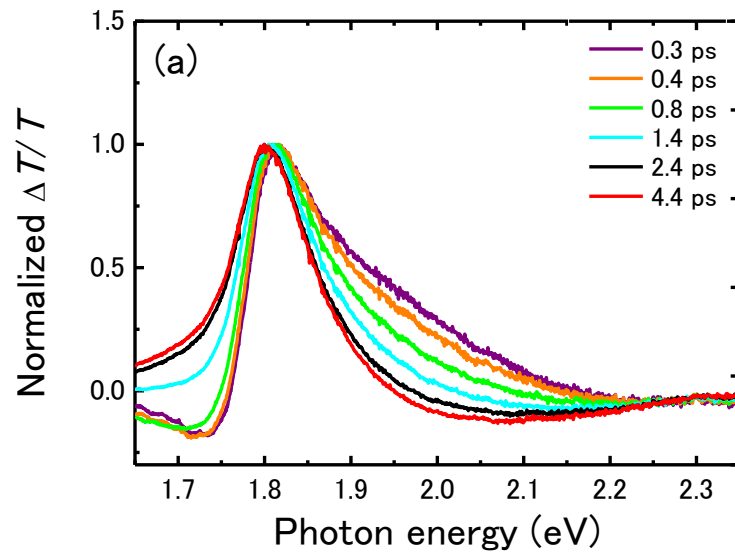


Fig. 2. XRD pattern of CsPbI₃.

Fig. 1 shows a typical optical absorption spectrum of the CsPbI₃ perovskite. A clear optical absorption shoulder can be observed at 1.8 eV, which corresponds to the excitonic transitions [41, 46]. Fig. 2 shows the X-ray diffraction (XRD) pattern of the CsPbI₃ perovskite, which confirms that the crystal structure of the CsPbI₃ is cubic phase. Special care was taken to ensure stability of the crystal phase in the CsPbI₃ perovskite films, as described in details in our previous paper [39]. Thin films of a polymer poly(methyl methacrylate), PMMA, were coated on the sample surfaces in order to encapsulate the samples from air.



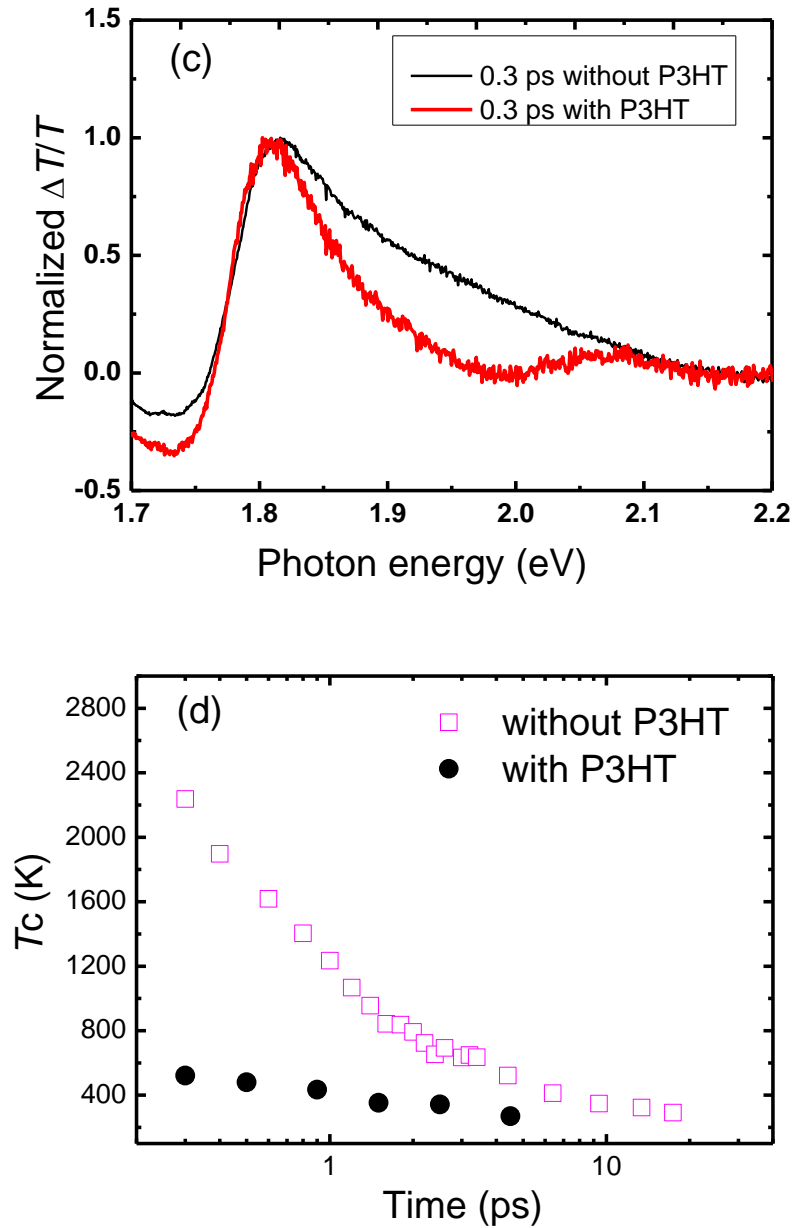


Fig. 3. Normalized TA spectra of CsPbI₃/Al₂O₃ for times from 0.1 ps to 4.4 ps [39] without P3HT (a) and with P3HT (b) as a hole extraction layer for times from 0.1 ps to 4.5 ps. (c) Comparison of normalized TA spectra at 0.3 ps for CsPbI₃/Al₂O₃ without and with P3HT (the photoexcited carrier density is $1.3 \times 10^{18} \text{ cm}^{-3}$). (d) The change in T_C against time for CsPbI₃/Al₂O₃ without and with

P3HT. For the TA spectra measurements, the pump light wavelength is 470 nm (pump energy is 2.6 eV) and the photoexcited carrier density is $1.3 \times 10^{18} \text{ cm}^{-3}$.

For the TA measurement, the pump light wavelength is 470 nm and its photon energy is 2.6 eV, which is larger than the bandgap 1.8 eV of CsPbI₃. Fig. 3(a) shows the normalized TA spectra of CsPbI₃/Al₂O₃ for times from 0.3 ps to 4.4 ps, where photoexcited carrier density is $1.3 \times 10^{18} \text{ cm}^{-3}$. Since no electrons or holes are expected to be transferred from CsPbI₃ to Al₂O₃, the intrinsic hot carrier relaxation dynamics in CsPbI₃ can be studied first. The detailed analyses of the TA spectra have been carried out in our previous paper [39]. The bleaching peak at 1.8 eV corresponds to the optical absorption peak of CsPbI₃. The negative TA peak just below the bandgap (1.75 eV) is due to the interplay between bandgap renormalization and the hot-carrier distribution [39]. We have shown that the distribution of the carriers for times longer than 0.3 ps are in quasi-thermal equilibrium and depend only on an effective carrier temperature T_C [39]. T_C can be calculated by fitting the TA spectra above the band edge (between 1.93 eV and 2.1 eV) to a Boltzmann distribution, i.e., $\Delta T/T[E > 1.9 \text{ eV}] \propto e^{-(E-E_f)/(K_B T_C)}$, where E_f is the quasi-Fermi energy and K_B is the Boltzmann constant [39–41]. Fig. 3(d) shows the time dependence of T_C of the CsPbI₃ perovskite, which is determined by fitting the TA spectra of Fig. 3(a) with the Boltzmann distribution [39]. Fast and slow processes are observed for hot carriers cooling down to the lattice temperature (i.e., the room temperature) in the CsPbI₃ perovskite. The initial fast hot carrier cooling occurs on a sub-ps time scale is followed by a much slower hot carrier cooling on a time scale of about 20 ps, which is considered to result from a hot phonon bottleneck effect [39,41]. One interesting question is whether the slow hot carrier cooling is possible or not using the solar illumination. To answer this question, we estimate the possible photoexcited carrier density in the absorber by 1 sun solar illumination. The photon flux of 1 sun (AM 1.5G) solar spectrum is shown

in Fig. S2(a), and the integrated photon flux from 300 nm to 470 nm of the AM 1.5G solar spectrum is shown in Fig. S2 (b) in the supporting information. The total photons from 300 nm to 470 nm of the AM1.5G solar spectrum could excite hot carriers under the similar experimental condition used in this study. From Fig. S2(b), we can know that the total photon flux from 300 nm to 470 nm is about $2.2 \times 10^{16} \text{ cm}^{-2}/\text{s}$. If we assume that all of these photons could be absorbed by the CsPbI₃ layer (thickness is 300 nm here), then the photoexcited hot carrier density is estimated to be $7 \times 10^{20} \text{ cm}^{-3}/\text{s}$, which is two orders larger than that necessary for slow hot carrier cooling ($7 \times 10^{18} \text{ cm}^{-3}$). Even if part of the light (e.g., 20%) is considered to transmit from the CsPbI₃ layer, the photoexcited hot carrier density is still so large that the hot carriers can relax slowly in a time scale of a few ten ps or longer than it. These results suggest that the slow hot carrier cooling in CsPbI₃ could occur for standard solar illumination.

Fig. 3(b) shows the normalized TA spectra of CsPbI₃/Al₂O₃ covered with P3HT from 0.3 ps to 4.5 ps for photoexcited carrier density of $1.3 \times 10^{18} \text{ cm}^{-3}$. A remarkable change occurs in the TA spectra of CsPbI₃ when P3HT is used as a hole extraction layer. The band tail at the higher energy side of bandgap due to ‘hot-carrier distribution’ cannot be observed anymore when P3HT is applied on CsPbI₃ as a hole extracting layer. This can be clearly observed by comparing the normalized TA spectra of CsPbI₃ with and without P3HT at 0.3 ps as shown in Fig. 3(c). As shown in Fig. 3(b), two very weak bleaching peaks can be observable at about 2.07 eV and 2.25 eV, respectively. The two peaks do not shift versus time and their intensities decay within 1 ps. Compared with the TA spectra of P3HT as shown in Fig. S3 in the supporting information, these bleaching peaks can be assigned to TA signals originating from P3HT [47,48]. In the TA measurements, the pump light was irradiated from the Al₂O₃/CsPbI₃ side of the sample. Thus, almost all the pump light was absorbed by the CsPbI₃ layer and only a small amount of light

passing through the CsPbI₃ could be absorbed by the P3HT layer. The very weak TA signals at 2.07 eV and 2.25 eV result from the optical absorption of the remaining small part of the initial pump light transmitted to P3HT. Most of the incident light beam is indeed absorbed by the CsPbI₃ layer. According to the band alignment diagrams of the CsPbI₃ and the P3HT as shown in Fig. S4 in the supporting information, photoexcited holes in CsPbI₃ can transfer to P3HT. By comparing the normalized TA spectra of only P3HT and those of CsPbI₃ on Al₂O₃ substrates with P3HT as shown in Fig. S5, we clearly observe that there is no TA signal from P3HT when the photon energy of the probe light is less than 1.95 eV. Then, even if some of the transmitted light of the CsPbI₃ layer is absorbed by P3HT, the TA spectra of P3HT do not have any influence on the disappearance of the hot carrier bleach (i.e., band tail broadening) in CsPbI₃ in the presence of P3HT. Therefore, the disappearance of the hot carrier bleach in CsPbI₃ in the presence of P3HT suggests ultrafast carrier cooling or charge transfer occurs in CsPbI₃ when P3HT exists.

Our interpretation is that the ultrafast hot hole transfer from CsPbI₃ to P3HT which occurs within a few 100 fs, deeply affects the hot carrier cooling regime. Fig. 3 (d) shows the change in the hot carrier temperature T_C against time for CsPbI₃/Al₂O₃ with and without P3HT, in which the photoexcited carrier density is $1.3 \times 10^{18} \text{ cm}^{-3}$. It can be clearly observed that T_C indeed significantly decreases from over 2000 K to about 500 K at 0.3 ps in the case of P3HT existing. This result means that the hot carriers cool down on a time scale of 300 fs when the P3HT hole extraction layer is added. The remaining TA signal thus mostly originates from the band edge electrons when P3HT is deposited on CsPbI₃. As shown in Fig. 4, a hot carrier bleach in TA spectrum (i.e., broadening in the high-energy tail) very similar to the one in CsPbI₃/Al₂O₃, can be observed as well in CsPbI₃/TiO₂ (CsPbI₃ deposited on mesoporous TiO₂). This result further confirms that the ultrafast carrier relaxation in CsPbI₃/Al₂O₃ with P3HT is primarily driven by hole extraction. Hot carriers

in CsPbI₃ do not relax so fast if the electron extracting layer of TiO₂ is used instead (Fig. 4). The mechanism for charge transfer dynamics from an inorganic semiconductor to an organic semiconductor is more complicated compared to that of the charge transfer at the inorganic semiconductor/inorganic semiconductor interfaces and needs to be studied systematically and deeply. It is considered that the charge transfer dynamics could be affected by the energetic force, wave function coupling at the inorganic semiconductor/organic semiconductor interface and the density of the charge transfer (CT) states in the organic semiconductor as reported in the ZnO/P3HT system [49]. Therefore, we think that the ultrafast hot hole extraction from CsPbI₃ to P3HT observed in our experiments suggests a possibility of the strong wave function coupling between the CsPbI₃ hot holes and the hot exciton charge transfer (CT) states in P3HT. Detailed studied about the mechanism is under progress and will be published elsewhere.

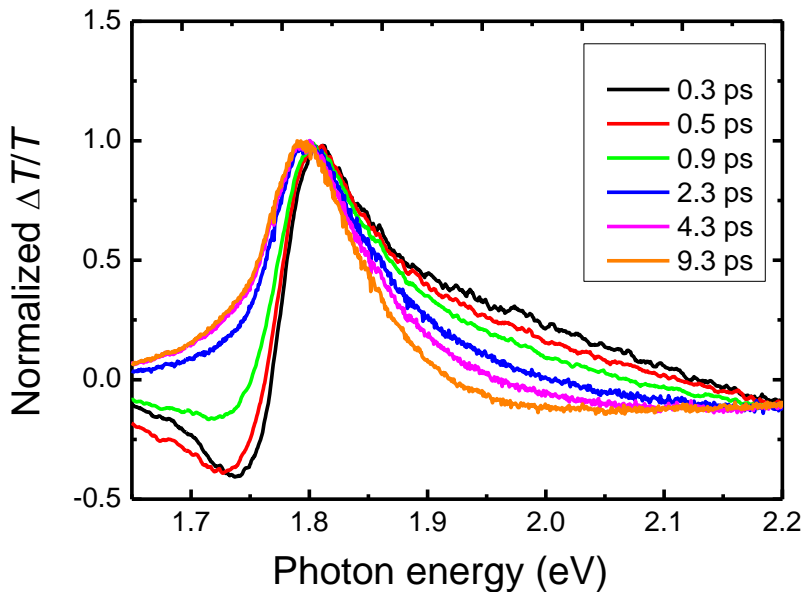


Fig. 4. Normalized TA spectra of CsPbI₃/TiO₂ for times from 0.3 ps to 9.3 ps (the photoexcited carrier density is $1.3 \times 10^{18} \text{ cm}^{-3}$).

Finally, provided that both electron and hole hot carrier populations are simultaneously generated after the initial pulse excitation, one may wonder how the efficient hot hole extraction by P3HT may in turn affect the hot electron cooling in CsPbI₃. A possible explanation is that through efficient electron-hole interactions, hot electrons may transfer their excess energy to the holes before extraction. The hot hole transfer to P3HT would thus indirectly help removing the excess energy of the electron population as well, in a manner analogous to the Auger electron-hole energy transfer in other semiconductors [50,51]. This picture is consistent with the experimental results shown in Fig. 3(b), where all hot carriers (both hot holes and hot electrons) seem to relax within a few 100 fs when P3HT is used as a contact layer. Thus, we propose that hot hole transfer to the P3HT layer can both depopulate the hot holes and the hot electrons, the latter as a result of electron-hole interactions, resulting in an overall reduction of energy losses through lattice thermalization.

4. Conclusions

In conclusion, we have clarified the hot carrier cooling dynamics in CsPbI₃ perovskite using Al₂O₃, P3HT and TiO₂ selective contacts. We observe that hot carriers cool slowly in CsPbI₃ perovskite on Al₂O₃ or TiO₂ to reach the room temperature in about 20 ps for the photoexcited carrier density of $1.3 \times 10^{18} \text{ cm}^{-3}$, which originates from a bottleneck of the carrier-phonon interactions. Most importantly, we find that hot holes in CsPbI₃ can be transferred through an ultrafast process to P3HT within a few 100 fs. On the other hand, simultaneous efficient hot electron cooling can be expected in CsPbI₃ by efficient transfer of the energy of electrons to hot holes. Our findings shed light on the potential application of CsPbI₃ to hot carrier solar cells.

Acknowledgments

This work was supported by the CREST program of Japan Science and Technology Agency (JST). The authors thank Ye Yang greatly for his very helpful discussions on the experimental results.

References

- [1] W.S. Yang, B.-W. Park, E.H. Jung, N.J. Jeon, Y.C. Kim, D.U. Lee, S.S. Shin, J. Seo, E.K. Kim, J.H. Noh, S.I. Seok, *Science*, 356 (2017) 1376-1379.
- [2] H.S. Jung, N.-G. Park, *Small*, 11 (2015) 2-2.
- [3] M.A. Green, A. Ho-Baillie, H.J. Snaith, *Nature Photon.*, 8 (2014) 506-514.
- [4] N.J. Jeon, J.H. Noh, Y.C. Kim, W.S. Yang, S. Ryu, S.I. Seok, *Nat Mater*, 13 (2014) 897-903.
- [5] M. Liu, M.B. Johnston, H.J. Snaith, *Nature*, 501 (2013) 395-398.
- [6] H. Zhou, Q. Chen, G. Li, S. Luo, T.-b. Song, H.-S. Duan, Z. Hong, J. You, Y. Liu, Y. Yang, *Science*, 345 (2014) 542-546.
- [7] J. Burschka, N. Pellet, S.-J. Moon, R. Humphry-Baker, P. Gao, M.K. Nazeeruddin, M. Grätzel, *Nature*, 499 (2013) 316-319.
- [8] G.E. Eperon, V.M. Burlakov, A. Goriely, H.J. Snaith, *ACS Nano*, 8 (2014) 591-598.
- [9] J.-H. Im, J. Chung, S.-J. Kim, N.-G. Park, *Nanoscale Res. Lett.*, 7 (2012) 353.
- [10] H.-S. Kim, C.-R. Lee, J.-H. Im, K.-B. Lee, T. Moehl, A. Marchioro, S.-J. Moon, R. Humphry-Baker, J.-H. Yum, J.E. Moser, M. Grätzel, N.-G. Park, *Sci. Rep.*, 2 (2012) 591.
- [11] M.M. Lee, J. Teuscher, T. Miyasaka, T.N. Murakami, H.J. Snaith, *Science*, 338 (2012) 643-647.

- [12] V. Gonzalez-Pedro, E.J. Juarez-Perez, W.-S. Arsyad, E.M. Barea, F. Fabregat-Santiago, I. Mora-Sero, J. Bisquert, *Nano Lett.*, 14 (2014) 888-893.
- [13] J.H. Noh, S.H. Im, J.H. Heo, T.N. Mandal, S.I. Seok, *Nano Lett.*, 13 (2013) 1764-1769.
- [14] N.-G. Park, *J. Phys. Chem. Lett.*, 4 (2013) 2423-2429.
- [15] J.T.-W. Wang, J.M. Ball, E.M. Barea, A. Abate, J.A. Alexander-Webber, J. Huang, M. Saliba, I. Mora-Sero, J. Bisquert, H.J. Snaith, R.J. Nicholas, *Nano Lett.*, 14 (2014) 724-730.
- [16] A. Abate, M. Saliba, D.J. Hollman, S.D. Stranks, K. Wojciechowski, R. Avolio, G. Grancini, A. Petrozza, H.J. Snaith, *Nano Lett.*, 14 (2014) 3247-3254.
- [17] A. Amat, E. Mosconi, E. Ronca, C. Quarti, P. Umari, M.K. Nazeeruddin, M. Grätzel, F. De Angelis, *Nano Lett.*, 14 (2014) 3608-3616.
- [18] Q. Chen, H. Zhou, T.-B. Song, S. Luo, Z. Hong, H.-S. Duan, L. Dou, Y. Liu, Y. Yang, *Nano Lett.*, 14 (2014) 4158-4163.
- [19] X. Wen, A. Ho-Baillie, S. Huang, R. Sheng, S. Chen, H.-c. Ko, M.A. Green, *Nano Lett.*, 15 (2015) 4644-4649.
- [20] S. Ye, W. Sun, Y. Li, W. Yan, H. Peng, Z. Bian, Z. Liu, C. Huang, *Nano Lett.*, 15 (2015) 3723-3728.
- [21] A. Yella, L.-P. Heiniger, P. Gao, M.K. Nazeeruddin, M. Grätzel, *Nano Lett.*, 14 (2014) 2591-2596.
- [22] W. Zhang, M. Anaya, G. Lozano, M.E. Calvo, M.B. Johnston, H. Míguez, H.J. Snaith, *Nano Lett.*, 15 (2015) 1698-1702.
- [23] G. Hodes, *Science*, 342 (2013) 317-318.
- [24] H.J. Snaith, *J. Phys. Chem. Lett.*, 4 (2013) 3623-3630.

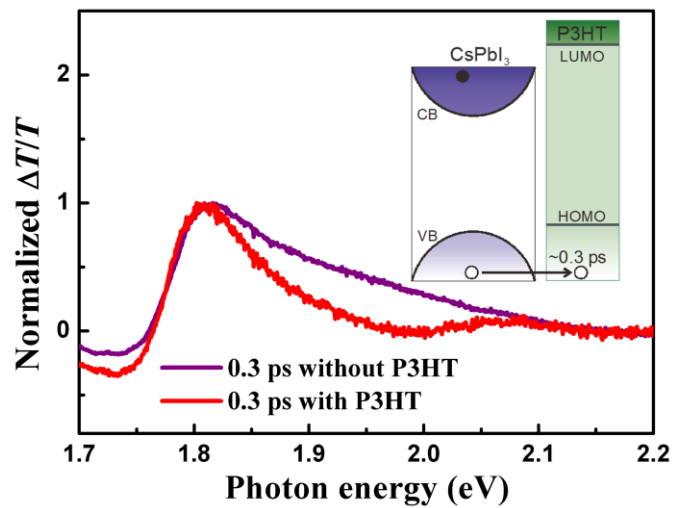
- [25] S. Sun, T. Salim, N. Mathews, M. Duchamp, C. Boothroyd, G. Xing, T.C. Sum, Y.M. Lam, *Energy Environ. Sci.*, 7 (2014) 399-407.
- [26] S.D. Stranks, G.E. Eperon, G. Grancini, C. Menelaou, M.J.P. Alcocer, T. Leijtens, L.M. Herz, A. Petrozza, H.J. Snaith, *Science*, 342 (2013) 341-344.
- [27] G. Xing, N. Mathews, S. Sun, S.S. Lim, Y.M. Lam, M. Grätzel, S. Mhaisalkar, T.C. Sum, *Science*, 342 (2013) 344-347.
- [28] S. De Wolf, J. Holovsky, S.-J. Moon, P. Löper, B. Niesen, M. Ledinsky, F.-J. Haug, J.-H. Yum, C. Ballif, *J. Phys. Chem. Lett.*, 5 (2014) 1035-1039.
- [29] T.S. Ripolles, K. Nishinaka, Y. Ogomi, Y. Miyata, S. Hayase, *Sol. Energ. Mat. Sol. Cells*, 144 (2016) 532-536.
- [30] G.E. Eperon, G.M. Paterno, R.J. Sutton, A. Zampetti, A.A. Haghighirad, F. Cacialli, H.J. Snaith, *J. Mater. Chem. A*, 3 (2015) 19688-19695.
- [31] R.E. Beal, D.J. Slotcavage, T. Leijtens, A.R. Bowring, R.A. Belisle, W.H. Nguyen, G.F. Burkhard, E.T. Hoke, M.D. McGehee, *J. Phys. Chem. Lett.*, 7 (2016) 746-751.
- [32] M. Kulbak, D. Cahen, G. Hodes, *J. Phys. Chem. Lett.*, 6 (2015) 2452-2456.
- [33] L. Protesescu, S. Yakunin, M.I. Bodnarchuk, F. Krieg, R. Caputo, C.H. Hendon, R.X. Yang, A. Walsh, M.V. Kovalenko, *Nano Lett.*, 15 (2015) 3692-3696.
- [34] S. Dastidar, D.A. Egger, L.Z. Tan, S.B. Cromer, A.D. Dillon, S. Liu, L. Kronik, A.M. Rappe, A.T. Fafarman, *Nano Lett.*, 16 (2016) 3563-3570.
- [35] A. Swarnkar, A.R. Marshall, E.M. Sanehira, B.D. Chernomordik, D.T. Moore, J.A. Christians, T. Chakrabarti, J.M. Luther, *Science*, 354 (2016) 92-95.
- [36] R.T. Ross, A.J. Nozik, *J. Appl. Phys.*, 53 (1982) 3813-3818.
- [37] O.D. Mücke, M. Wegener, *Appl. Phys. Lett.*, 73 (1998) 569-571.

- [38] M. Elsässer, S.G. Hense, M. Wegener, *Appl. Phys. Lett.*, 70 (1997) 853-855.
- [39] Q. Shen, T.S. Ripolles, J. Even, Y. Ogomi, K. Nishinaka, T. Izuishi, N. Nakazawa, Y. Zhang, C. Ding, F. Liu, T. Toyoda, K. Yoshino, T. Minemoto, K. Katayama, S. Hayase, *Appl. Phys. Lett.*, 111 (2017) 153903.
- [40] M.B. Price, J. Butkus, T.C. Jellicoe, A. Sadhanala, A. Briane, J.E. Halpert, K. Broch, J.M. Hodgkiss, R.H. Friend, F. Deschler, *Nat. Commun.*, 6 (2015) 8420.
- [41] Y. Yang, D.P. Ostrowski, R.M. France, K. Zhu, J. van de Lagemaat, J.M. Luther, M.C. Beard, *Nature Photon.*, 10 (2016) 53-59.
- [42] Q. Shen, Y. Ogomi, B.-w. Park, T. Inoue, S.S. Pandey, A. Miyamoto, S. Fujita, K. Katayama, T. Toyoda, S. Hayase, *Phys. Chem. Chem. Phys.*, 14 (2012) 4605-4613.
- [43] Q. Shen, Y. Ogomi, S.K. Das, S.S. Pandey, K. Yoshino, K. Katayama, H. Momose, T. Toyoda, S. Hayase, *Phys. Chem. Chem. Phys.*, 15 (2013) 14370-14376.
- [44] Q. Shen, Y. Ogomi, J. Chang, S. Tsukamoto, K. Kukihara, T. Oshima, N. Osada, K. Yoshino, K. Katayama, T. Toyoda, S. Hayase, *Phys. Chem. Chem. Phys.*, 16 (2014) 19984-19992.
- [45] Q. Shen, Y. Ogomi, J. Chang, T. Toyoda, K. Fujiwara, K. Yoshino, K. Sato, K. Yamazaki, M. Akimoto, Y. Kuga, K. Katayama, S. Hayase, *J. Mater. Chem. A*, 3 (2015) 9308-9316.
- [46] Y. Yang, Y. Yan, M. Yang, S. Choi, K. Zhu, J.M. Luther, M.C. Beard, *Nat. Commun.*, 6 (2015) 7961.
- [47] G. Grancini, D. Polli, D. Fazzi, J. Cabanillas-Gonzalez, G. Cerullo, G. Lanzani, *J. Phys. Chem. Lett.*, 2 (2011) 1099-1105.
- [48] T.M. Clarke, F.C. Jamieson, J.R. Durrant, *J. Phys. Chem. C*, 113 (2009) 20934-20941.
- [49] G.F. Wu, Z. Li, X. Zhang, and G. Lu, *J. Phys. Chem. Lett.*, 5 (2014) 2649-2656.

[50] H. Zhu, Y. Yang, K. Hyeon-Deuk, M. Califano, N. Song, Y. Wang, W. Zhang, O.V. Prezhdo, T. Lian, *Nano Lett.*, 14 (2014) 1263-1269.

[51] V.I. Klimov, D.W. McBranch, *Phys. Rev. Lett.*, 80 (1998) 4028-4031.

Graphical Abstract:



The band tail broadening at high energy side of the bandgap due to “hot-carrier distribution” in the TA spectrum of CsPbI₃ cannot be observed when P3HT exists, suggesting hot hole transfer from CsPbI₃ to P3HT.